

Magnetism and magnetic asphericity in NiFe alloys

Biplab Sanyal[‡] and Abhijit Mookerjee

S.N.Bose National Centre for Basic Sciences, JD Block, Sector 3, Salt Lake City,
Calcutta 700091, India

Abstract. We here study magnetic properties of $\text{Ni}_x\text{Fe}_{1-x}$ using Augmented space recursion technique coupled with tight-binding linearized muffin tin orbital method. Also the spectral properties of this alloy has been studied here.

PACS numbers: 71.20.-b, 71.23.-k, 71.20.Be, 71.15.-m

Keywords : Magnetism, alloys, augmented space recursion

1. Introduction

NiFe alloys have been extensively studied earlier. Experimental data have been available for decades. Neutron scattering has probed the local magnetic moments [1, 2, 3, 4, 5]. Theoretical approaches include the Hartree-Fock approaches of Hasegawa and Kanamori [6] and Kanamori [7]. These authors assumed the density of states to be steep models, and were therefore only qualitative. They used the coherent potential approach (CPA) of Velický *et al* [8] in order to describe disorder and configuration averaging. Mishra and Mookerjee [9] have used the Hartree-Fock model of Hasegawa and Kanamori but the averaged density of states was obtained from the augmented space technique based cluster CPA. Podgórný [10] studied NiFe using the supercell linearized muffin-tin orbitals method (LMTO) while Lipiński [11] applied the tight-binding LMTO-CPA.

[‡] Corresponding author. Fax : 0091 333343477, Phone : 0091 333583061, E-mail : biplab@boson.bose.res.in

NiFe alloys have interesting behaviour. The magnetic behaviour of Ni is anomalous in the sense that the local magnetic moment of Ni depends sensitively on its immediate surrounding. The local magnetic moment on a Ni atom depends upon the number of Ni neighbours it has. The CPA which replaces the random neighbourhood of an atom in a solid solution by an effective, averaged medium cannot reflect this behaviour. The aim of this communication is to study NiFe by the augmented space recursion (ASR) technique [12]. Recently we have shown that the ASR allows us to go beyond the CPA without violating the essential herglotz analytic properties and take into account the effect of local neighbourhood [13]. The ASR will be based on the TB-LMTO hamiltonian

$$\begin{aligned}
H &= \sum_{RL} \hat{C}_{RL} \mathcal{P}_{RL} + \sum_{RL} \sum_{R'L'} \hat{\Delta}_{RL}^{1/2} S_{RL,R'L'} \hat{\Delta}_{R'L'}^{1/2} \mathcal{T}_{RL,R'L'} \\
\hat{C}_{RL} &= C_{RL}^B + (C_{RL}^A - C_{RL}^B) n_R \\
\hat{\Delta}_{RL}^{1/2} &= \Delta_{RL}^{B1/2} + (\Delta_{RL}^{A1/2} - \Delta_{RL}^{B1/2}) n_R
\end{aligned} \tag{1}$$

Here \mathcal{P}_{RL} and $\mathcal{T}_{RL,R'L'}$ are projection and transfer operators in the hilbert space spanned by the tight binding basis $|RL\rangle$ and n_R is a random occupation variable which is 1 if the site R is occupied by an atom of the A type and 0 if not. The augmented space hamiltonian replaces the random occupation variable by operators M_R of rank 2. For models without any short-range order

$$\begin{aligned}
M_R &= x \mathcal{P}_{\uparrow}^R + (1-x) \mathcal{P}_{\downarrow}^R + \sqrt{x(1-x)} (\mathcal{T}_{\uparrow\downarrow}^R + \mathcal{T}_{\downarrow\uparrow}^R) \\
|\uparrow\rangle &= (\sqrt{x}|0\rangle + \sqrt{1-x}|1\rangle) \\
|\downarrow\rangle &= (\sqrt{1-x}|0\rangle - \sqrt{x}|1\rangle)
\end{aligned}$$

The ASR was carried out with LDA self-consistency. The computations included scalar relativistic corrections. The exchange potential of von Barth-Hedin was used. We

used the choice of flexible Wigner Seitz radii for Ni and Fe as suggested by Kudrnovský and Drchal [14] in order to ensure the atomic spheres to be neutral and avoid the calculation of the Madelung energy.

The recursion method then expresses the Green functions as continued fraction expansions. The continued fraction coefficients are exactly obtained upto eight levels and the terminator suggested by Luchini and Nex [15] is used to approximate the asymptotic part. The convergence of this procedure has been discussed by Ghosh *et al* [16]. The local charge densities are given by :

$$\rho_{\sigma}^{\lambda}(r) = (-1/\pi)\Im m \sum_L \int_{-\infty}^{E_F} dE \ll G_{LL}^{\lambda,\sigma}(r, r, E) \gg \quad (2)$$

Here λ is either A or B . The local magnetic moment is

$$m^{\lambda} = \int_{r < R_{WS}} d^3r [\rho_{\uparrow}(r) - \rho_{\downarrow}(r)]$$

We have also obtained the spectral densities and complex band structures for 50-50 Ni-Fe using the ASR in k-space as suggested by Biswas *et al* [17].

For high concentrations of Ni the alloy forms a face centred cubic solid solution. With decreasing Ni concentration, at the invar concentration of about 30%, the system undergoes a structural phase transition to a body centred cubic solid solution. At this transition there is a sharp decrease of Wigner-Seitz radius. This leads to larger overlap of the d -bands, and hence, using the Stoner criterion, a decrease of magnetization. We shall limit ourselves to the face centred cubic region beyond the invar concentration.

2. Results and Discussion

Figures 1(a) and (b) show the Ni and Fe partial density of states for Ni concentrations varying between 90 and 40 %. We note that the Ni densities hardly change with concentration, while the Fe densities change considerably. For the minority spin partial

densities on Fe, the structures below the Fermi energy do not change with concentration. The peak at around 0.0 Ryd grows with increasing Ni concentration. However, this structure is above the Fermi level and does not contribute to the magnetic moment. For the majority spin partial densities on Fe, the peak around -0.4 Ryd grows with increasing Ni concentration. This ensures that the Ni local magnetic moment remains almost concentration independent, while the Fe local moment increases with Ni concentration. Figure 2 shows the Ni and Fe moments as well as the average moment as functions of Ni concentration. The results agree rather well with earlier CPA results. In addition we have shown the experimental results on the average magnetic moment by Crangle and Halam [18] as well as the experimental data on local magnetic moments on Fe and Ni by Shull and Wilkinson [1], Collins *et al* [2] and Nishi *et al* [3]. The experimental data are reasonably reproduced, as well as CPA did earlier.

Both the CPA and our results indicate a slight increase of the Fe magnetic moment as the Ni concentration increases. The experimental data with its large error bars tell us little about this trend with certainty. The asphericity, which is measured by the ratio of the t_{2g} and e_g contributions to the magnetic moment, is shown in figure 3. The results indicate that the Ni moment distribution is highly anisotropic. The t_{2g} dominates the magnetization as well as the density of states peaks near the Fermi level. We also compare our results with neutron scattering experimental data of Brown *et al* [4] and Ito *et al* [5]. The asphericity trend with concentration is reproduced, but our average asphericities are slightly larger. The asphericity decreases with decreasing Ni concentration. The Fe moment distribution is almost spherical throughout the concentration range, with a slight decrease with decreasing Ni concentration. The average asphericity agrees reasonably well with experiment [4, 5].

Figures 4 (a) and (b) gives the spectral densities for k-vectors going from the Γ to

the X point for the e_g and t_{2g} bands. The results clearly show the splitting between the majority and minority spin bands. The imaginary part of the self-energy which measures the disorder scattering life-time, is clearly k -dependent and is more prominent at the X point and least at the Γ point. This is in contrast to the CPA calculations where the life-times are almost k -independent. Angle-resolved photoemission experiments show the spectral behaviour of alloys and the nature of fuzzy fermi surfaces can be obtained from Compton scattering and positron annihilation experiments. The complex bands are obtained from the peaks and widths in the spectral densities. These are shown in figure 5 (a) and (b). We note that the d -bands of Fe and Ni overlap considerably, and although the e_g and t_{2g} type bands are evident, they are broadened by disorder. The lines shown in figure 5 are to guide the eye. The statements made above based on the spectral functions are clearly seen in this figure. The Fermi level crosses the minority spin bands. These bands have considerable life-times and the Fermi surface should have this width associated with it. It should be interesting to look at the fuzzy Fermi surface experimentally.

NiFe alloys tend to exhibit short-ranged order. The augmented space recursion is ideally suited to take into account effects of short-ranged order. The formalism to include this has been introduced earlier by Mookerjee and Prasad [19] and applied to alloy systems by Saha *et al* [13]. We have carried out the calculation of the magnetic moment of the 50-50 NiFe alloy as a function of the Warren-Cowley short-ranged order parameter α . The magnetic moment of Fe is hardly affected by short-ranged order. However, in the region where $\alpha < 0$ indicating ordering, Ni is more likely to have Fe neighbours as compared to the case without short-ranged order. Here the magnetic moment on Ni increases. Similarly, when $\alpha > 0$, Ni atoms segregate and are less likely to have Fe as their neighbours and the Ni moment decreases. This is shown in figure

6. We conclude that extra moment is induced on Ni by Fe atoms in its vicinity. This induced moment on Ni is most sensitive to short-ranged order in the alloy.

References

- [1] Shull C G and Wilkinson M K 1955 *Phys. Rev.* **97** 304
- [2] Collins M F, Jones R V and Lowde R D 1962 *J. Phys. Soc. Japan* **17** B-III 19
- [3] Nishi M, Nakai Y and Kunitomi N 1974 *J. Phys. Soc. Japan* **37** 570
- [4] Brown P J, Deportes J and Ziebeck K R A 1991 *J. Physique* **1** 1529 ; Brown P J, Jassim I K, Neumann K U and Ziebeck K R A 1989 *Physica* **B161** 9
- [5] Ito Y, Akimitsu J, Matsui M and Chikazami S 1979 *J. Magn. Magn. Mat.* **10** 194.
- [6] Hasegawa H and Kanamori J 1971 *J. Phys. Soc. Japan* **31** 382 ; 1972 *J. Phys. Soc. Japan* **33** 1599
- [7] Kanamori J 1963 *Prog. Theor. Phys.* **30** 275
- [8] Velický B, Kirkpatrick S and Ehrenreich H 1968 *Phys. Rev.* **175** 747
- [9] Mishra A K and Mookerjee A 1990 *Int. J. Mod. Phys.* **B4** 605
- [10] Podgorný P 1990 *Acta Phys. Polon.* **A78** 941
- [11] Lipiński S 1993 *Int. J. Mod. Phys.* **B7** 965
- [12] Mookerjee A 1973 *J. Phys. C: Solid State Phys.* **6** L205 ; **6** 1340; Haydock R, Heine V and Kelly M J 1972 *J. Phys. C: Solid State Phys.* **5** 2845
- [13] Saha T, Dasgupta I and Mookerjee A 1996 *J. Phys.: Condens. Matter* **8** 1979
- [14] Kudrnovský J and Drchal V 1990 *Phys. Rev.* **B41** 7515
- [15] Luchini M U and Nex C M M 1987 *J. Phys. C: Solid State Phys.* **20** 3125
- [16] Ghosh S, Das N and Mookerjee A 1997 *J. Phys.: Condens. Matter* **9** 1701
- [17] Biswas P , Sanyal B, Fakhruddin M, Halder A, Mookerjee A and Ahmed M 1995 *J. Phys.: Condens. Matter* **7** 8569
- [18] Crangle J and Halam G C 1963 *Proc. Roy. Soc.* **A272** 119
- [19] Mookerjee A and Prasad R 1993 *Phys. Rev.* **B48** 17724

Figure Captions

Figure 1 (a) Partial densities of states at Ni sites. (b) Partial densities of states at Fe sites. The concentrations of Ni are shown as are the Fermi energies (vertical lines).

Figure 2 Magnetic moments on Fe and Ni sites and the averaged magnetic moment as functions of Ni concentration. The diamond marks indicate the experimental results of Crangle and Halam, the dashed points of Shull and Wilkinson, the square points of Collins and Lowde and the crossed points of Nishi *et al* .

Figure 3 Asphericity of moment distribution on Fe and Ni sites as functions of Ni

concentration. The cross marks indicate the neutron scattering results of Brown *et al* and Ito *et al* .

Figure 4 The spectral densities for (a) e_g and (b) t_{2g} states along the Γ to X direction for 50-50 FeNi. The bold curves are for the majority spins and the dotted curve for the minority spins. For both (a) and (b), the wave vectors of figures are (from top to bottom) $(1,0,0)$, $(0.75,0,0)$, $(0.5,0,0)$, $(0.25,0,0)$ and $(0,0,0)$ in units of $2\pi/a$, where a is the lattice constant.

Figure 5 Complex band structure for d -bands of 50-50 FeNi (a) For the majority spin bands (b) for the minority spin bands. The widths of the bands are marked and the lines are only to guide the eye.

Figure 6 The averaged magnetic moment and the magnetic moment of Ni as functions of the Warren-Cowley short-ranged order parameter for 50-50 NiFe.

Figure 1(a)

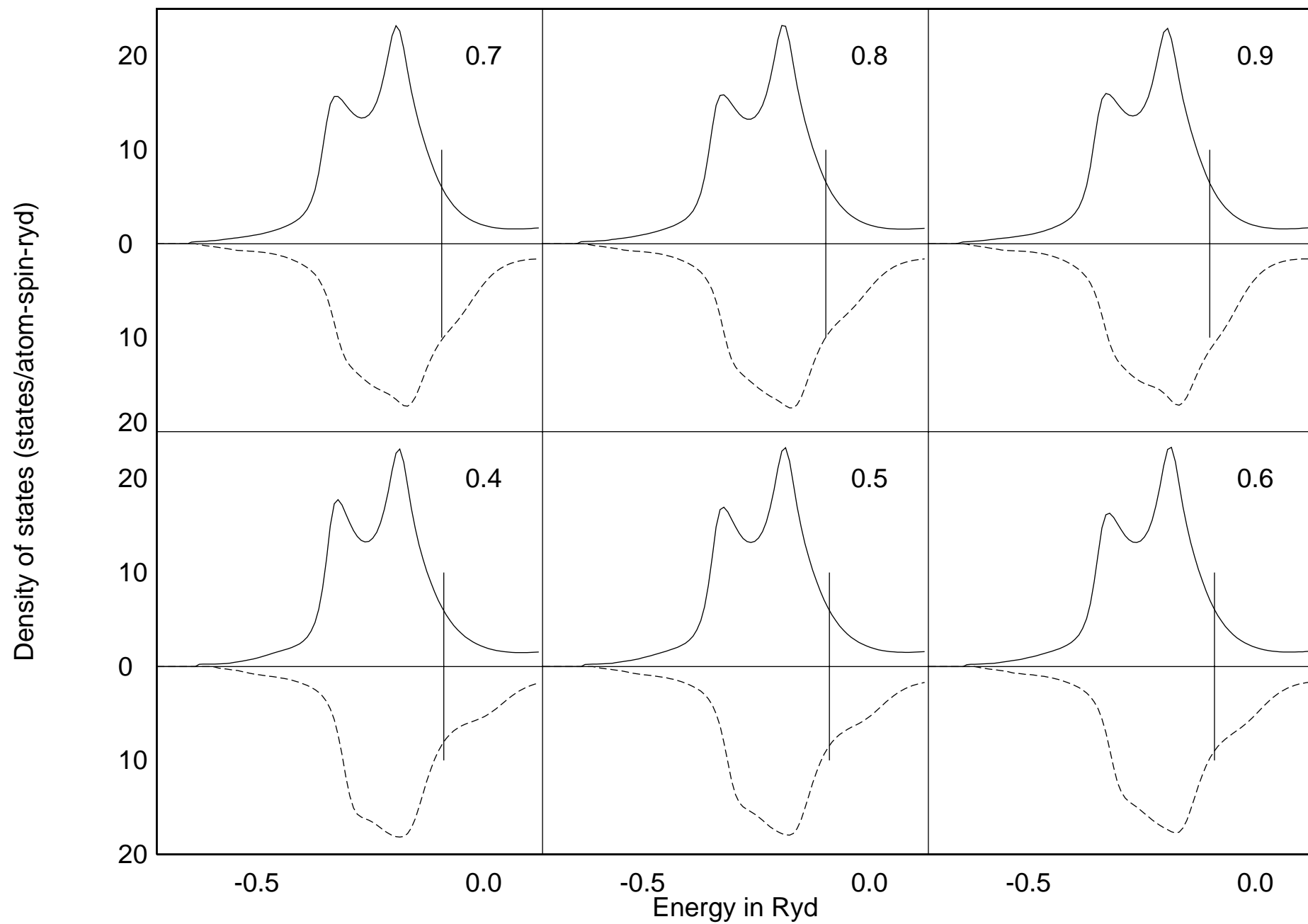


Figure 1(b)

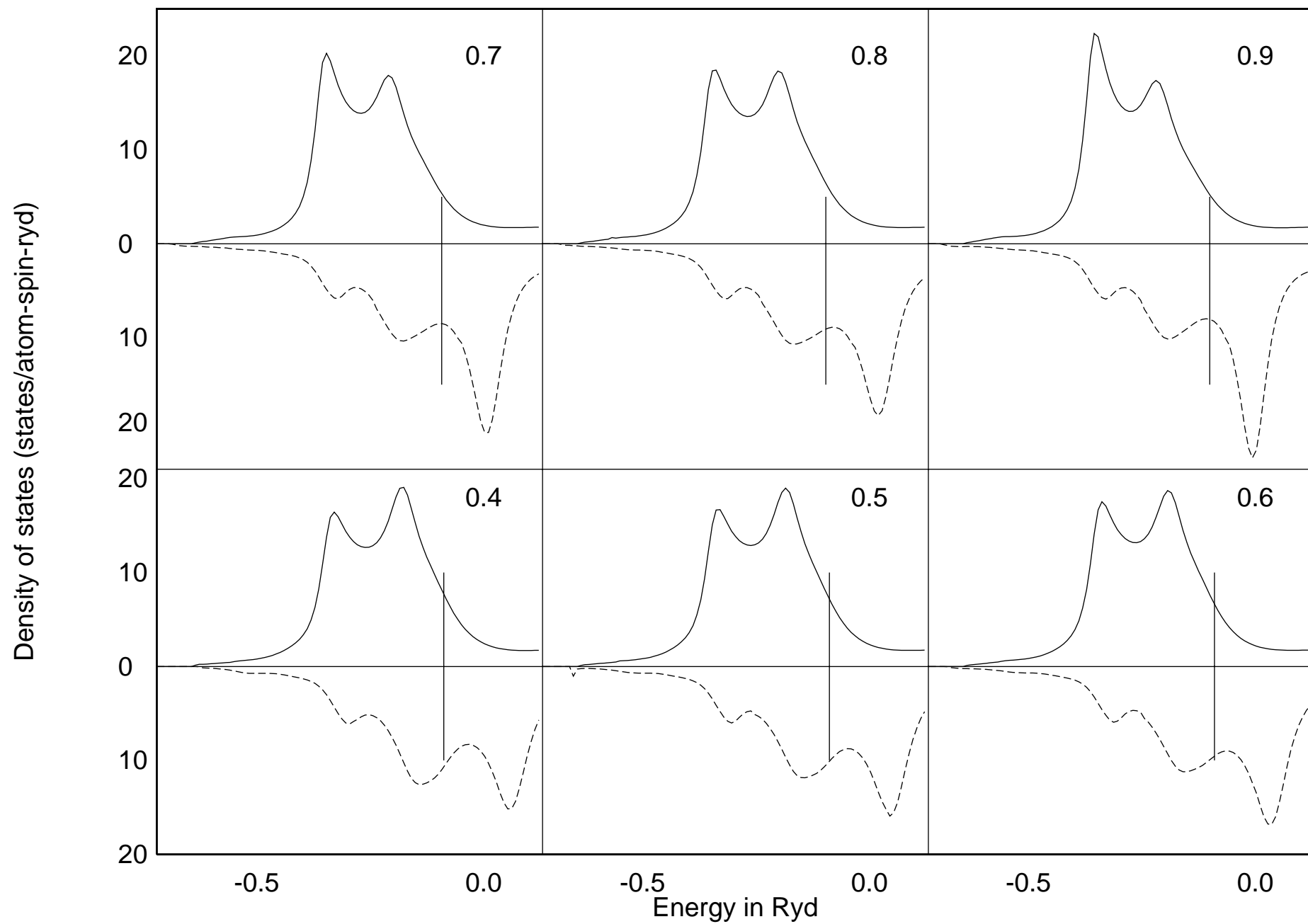


Figure 1(b)

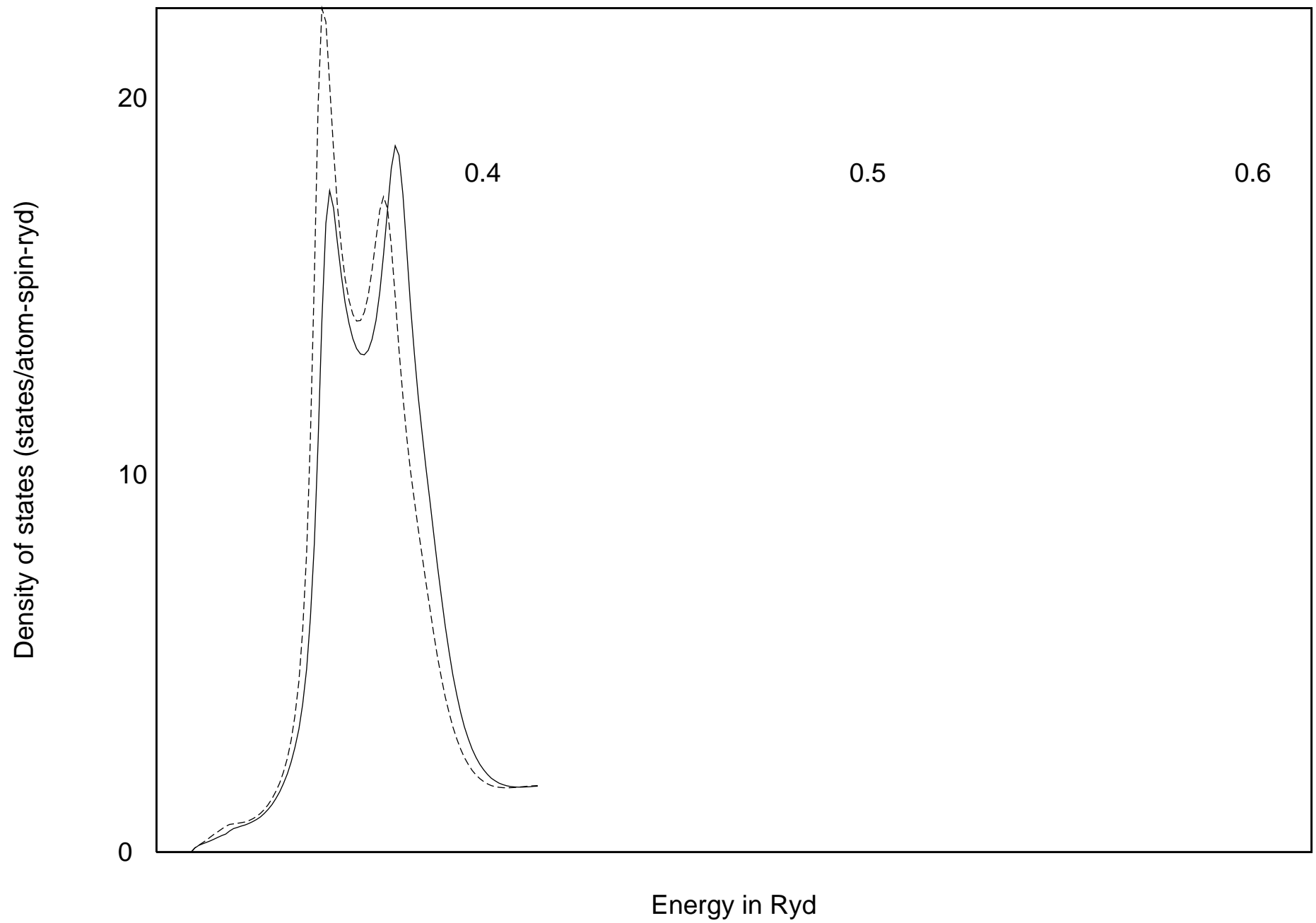


Figure 2

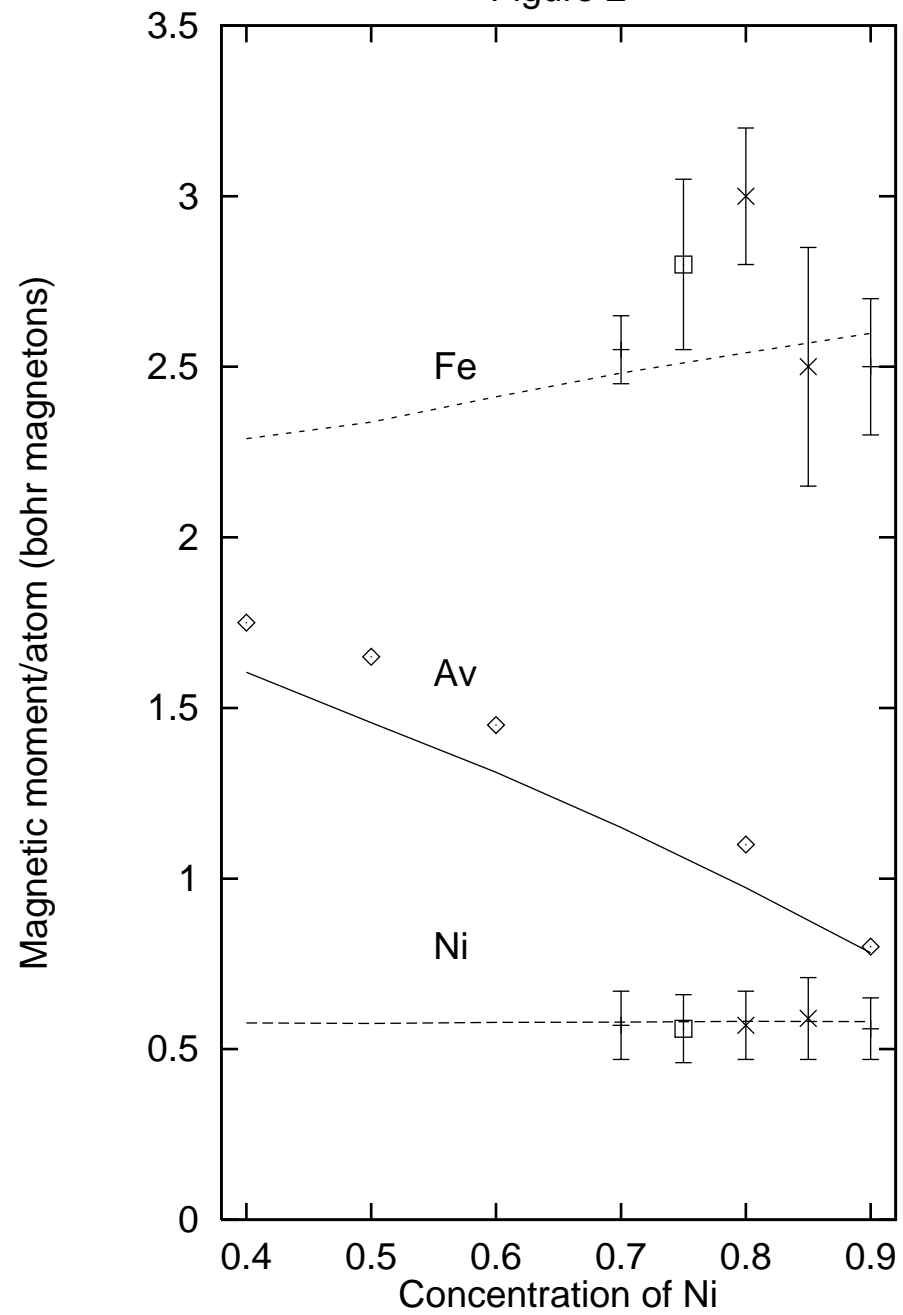
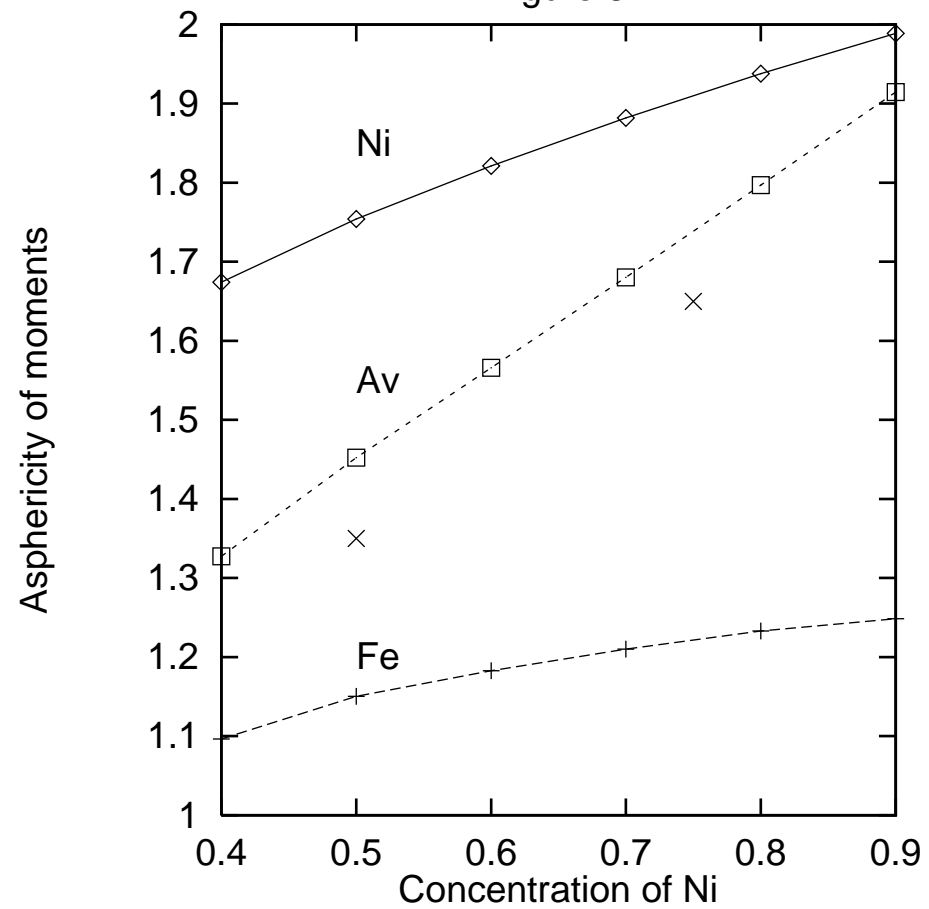
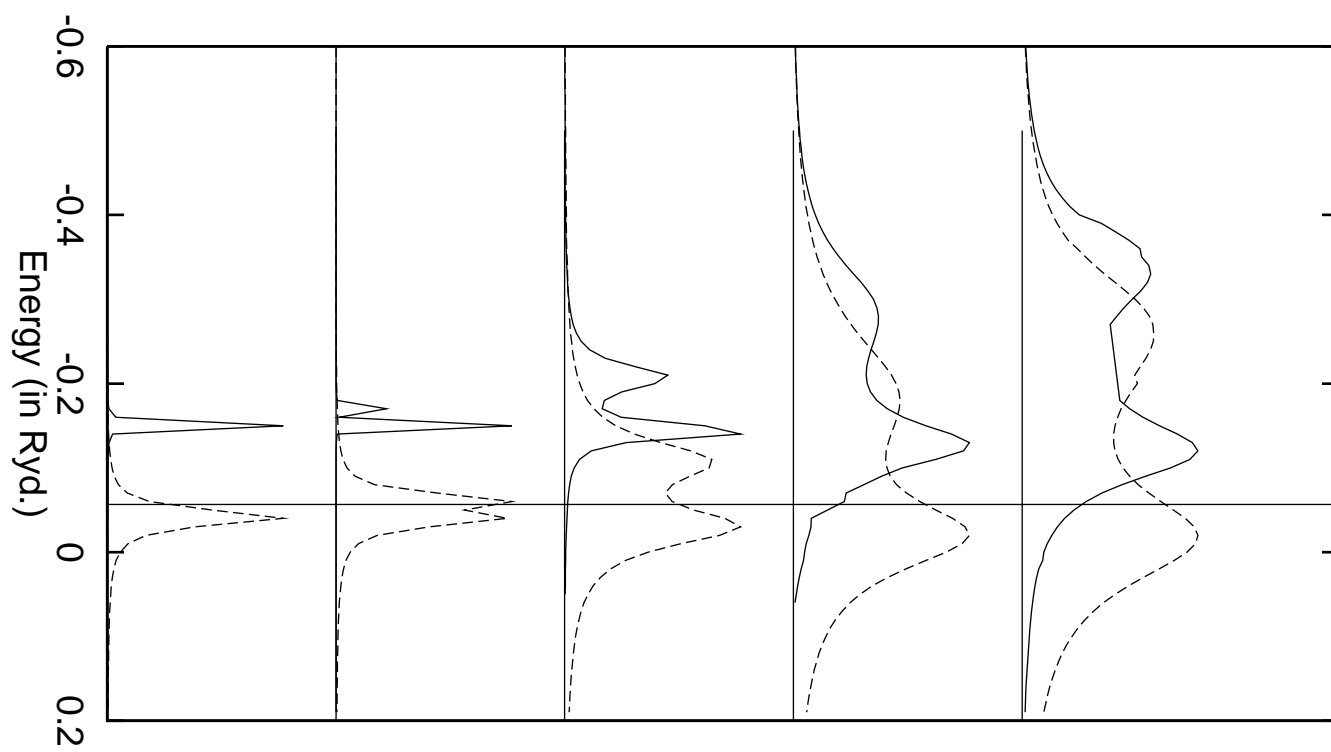


Figure 3



Spectral density (arbitrary units)



Spectral density (arbitrary units)

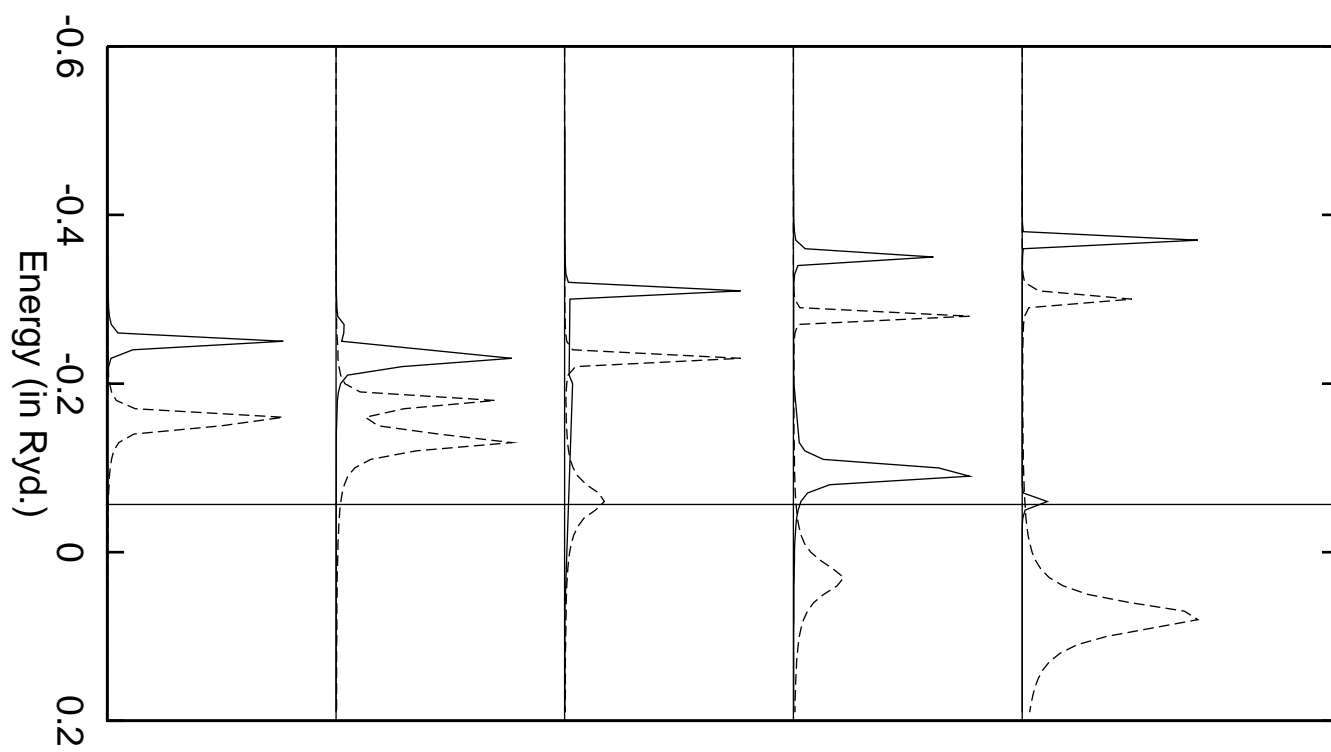


Figure 5(a)

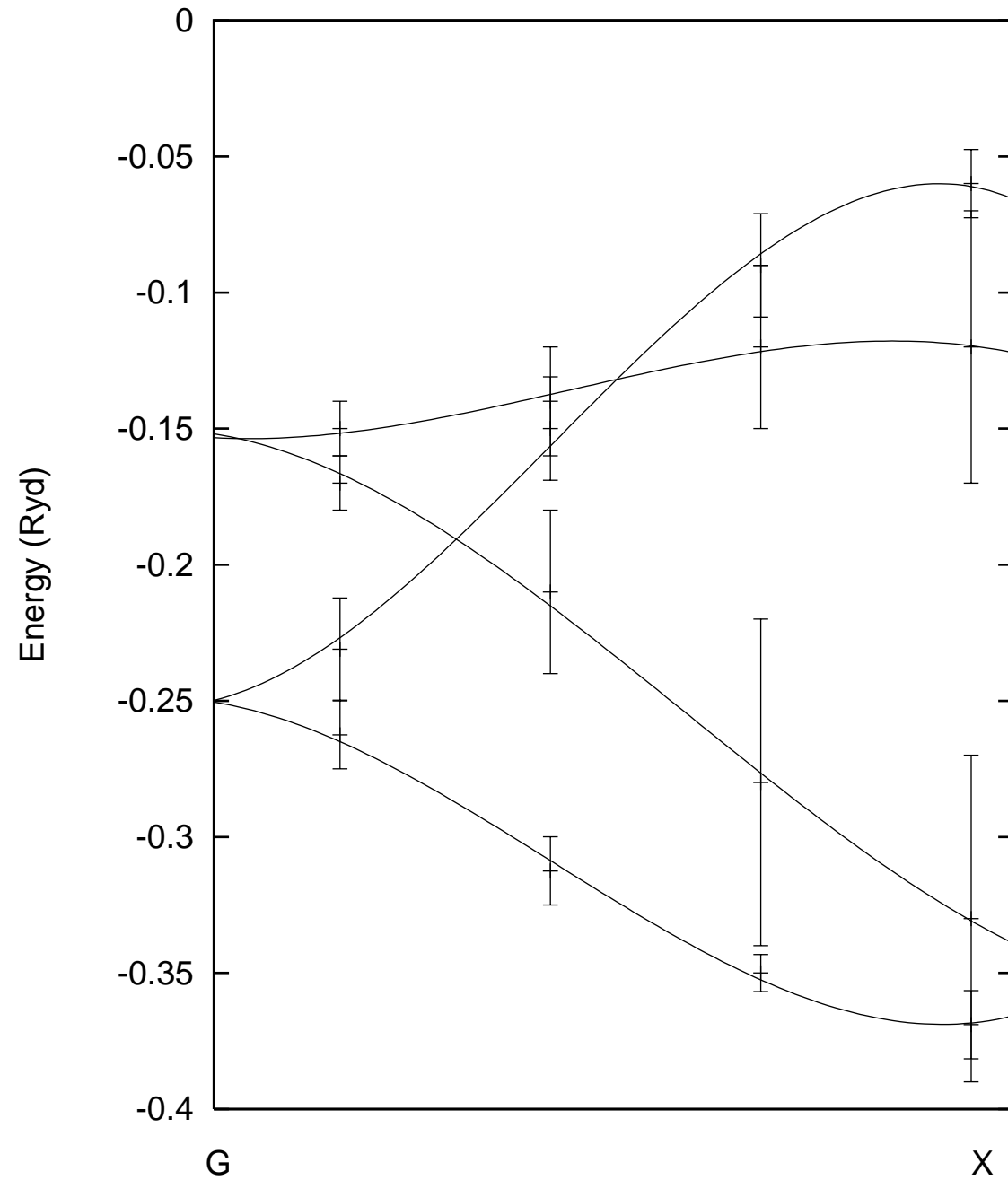


Figure 5(b)

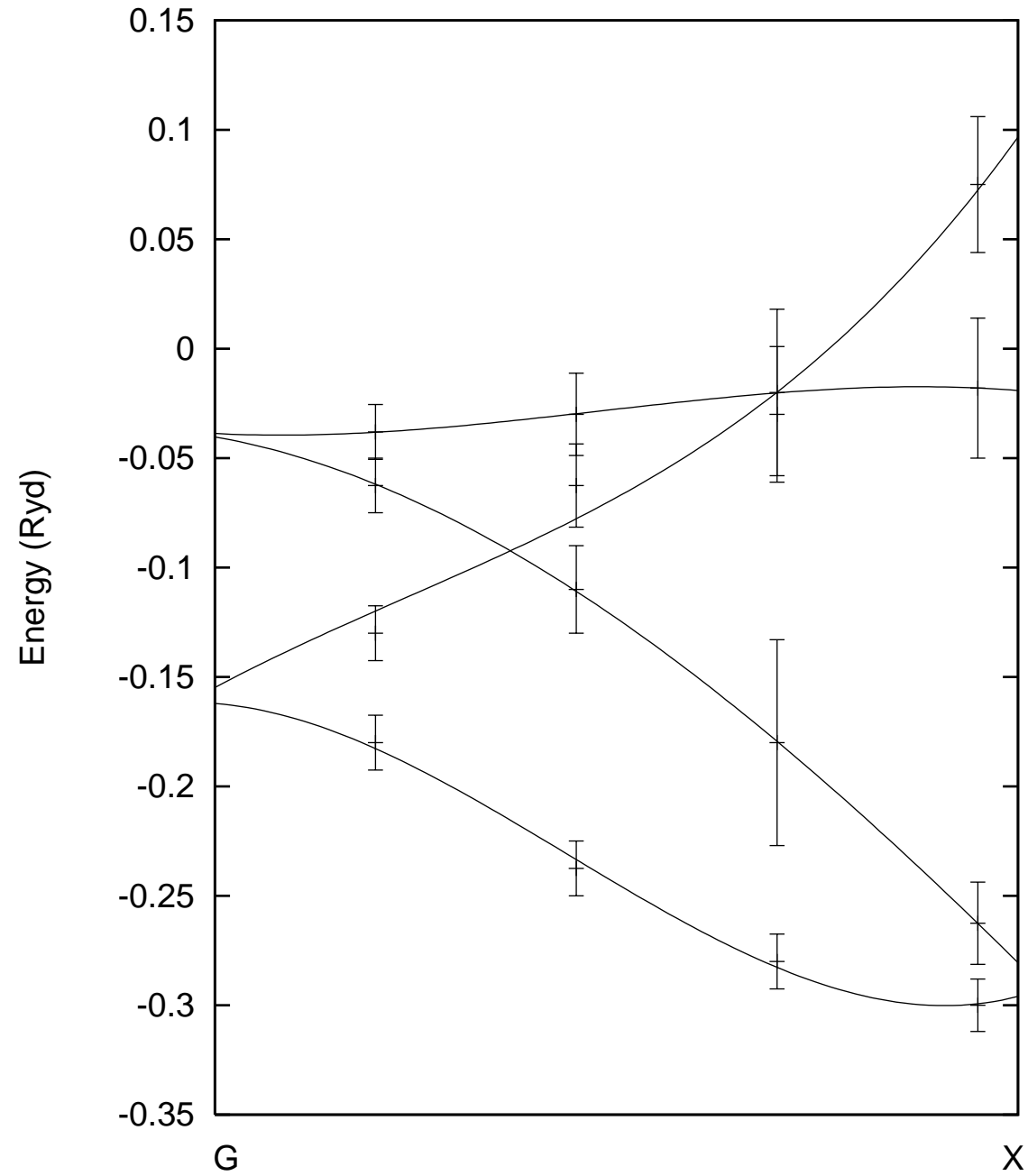


Figure 6

